NUKLEONIKA 2000;45(3):173–177

ORIGINAL PAPER

On the influence of a carbon solid on the properties of a helium plasma in a theta pinch discharge

Wolfgang Freese,
Hans-Joachim Kunze

Abstract A helium plasma produced in a 82 kJ theta pinch discharge has been seeded with carbon ions by a carbon solid rod positioned on the axis. The first shock front of the discharge ablates carbon atoms from the solid surface which are ionized and interact with the plasma. Some shock front properties (namely thickness, compression velocity and its shape) were analyzed with an ICCD-camera system taking 2-dimensional photos of the plasma continuum emitted along the axis with a time duration of 100 ns. While an influence on the shape was not found, the temporal behaviour was drastically changed when the rod was added. The shock front occurs earlier and compresses faster. An explanation remains to be given. Furthermore, the influence of the carbon impurities on the plasma parameters has been investigated by measuring the electron temperature and density by means of plasma spectroscopy comparing these results with those obtained from discharges in helium without rod. We found a decrease in the electron density about 500 ns after the shocked plasma has started to interact with the rod surface. Simultaneously increasing continuum emission and decreasing intensity of the HeII P_α line indicates a regime of recombination. No influence was found on the electron temperature.

Key words shock wave • spectroscopy • theta pinch

W. Freese✉, H.-J. Kunze
Institute for Experimental Physics V, Ruhr-University,
D-44780 Bochum, Germany,
Tel.: +49234/ 3225785, Fax: +49234/ 3194175,
e-mail: wolfgang.freese@megamos.de

Received: 31 January 2000, Accepted: 18 April 2000

Introduction

In former investigations of a 110 kJ theta pinch discharge in helium (at an initial pressure of 300 mTorr) a strong radiation of carbon impurities was observed. These impurities originate in the interaction of the plasma with the inner wall of the discharge chamber in the early stage of plasma formation. At maximum compression CIII and CIV lines were found near the axis, being a source for radiation losses. Going one step further we seeded a pure helium plasma with higher amounts of carbon by means of a carbon solid rod positioned on the axis. Carbon material ablated from the surface of the rod by the shocked plasma is expected to influence the plasma locally. At least, energy losses due to ablation processes, strong impurity radiation as well as recombination suggest a decrease of the electron temperature near the axis. Therefore, the magnetic piston following the shock would penetrate into a cold plasma region, if the delay between the shock and the piston is shorter than the energy diffusion time along the radius, i.e. if the temperature gradient along the radius does not change significantly until the piston reaches the axis. Further experiments with more emphasis on the time delay between the shock front and the piston (which can be controlled by means of the initial pressure and the main voltage) are necessary before the results may be safely extrapolated to population inversion conditions. As a beginning we focused our interest on the influ-

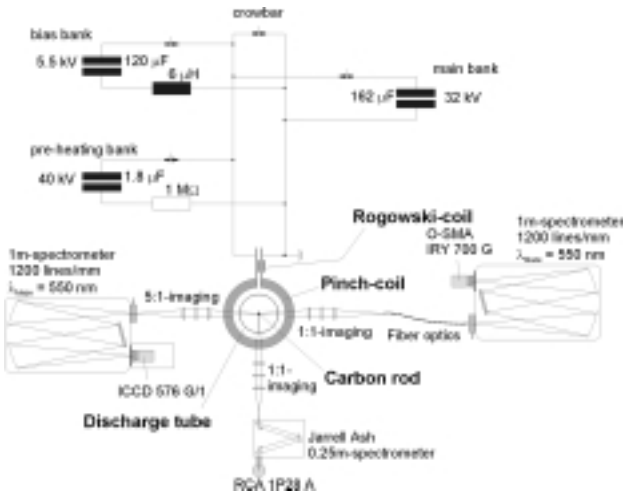

Fig. 1. Setup scheme of the theta pinch device.

ence of the carbon impurities on the dynamics of the discharge, namely on the shock front thickness and velocity, as well as on the dependence of the temperature and density of the electrons on the presence of the carbon impurities in the discharge.

In this paper we present first results of our investigations on the shock wave structure and its interaction with the carbon rod. End-on photos of an ICCD-camera were used to derive the thickness d_{shock} and the compression velocity v_{shock} of the shock front and to proof its cylindrical symmetry. The electron density and temperature was measured side-on with an OMA-system via fibre optics giving mean values along the radius. All results are compared with those obtained from discharges without the rod on the axis.

Experimental setup

Since the theta pinch device was developed in the early days of fusion research, the setup has been described in many papers with more or less modified details (see, e.g., [1, 6, 9, 15]). The specifications of the theta pinch device at the Ruhr-University, Bochum as operated at present are as follows (see Fig. 1 and [7, 10]).

The discharge glass tube (length 2 m, inner radius 15 cm) is filled with helium at an initial pressure of 250 mTorr. The helium gas is weakly ionized by means of an rf-discharge 250 µs before the main capacitor bank is discharged (at t = 0 µs). In order to achieve a field-reversed configuration the bias-capacitor (C_{bias} = 120 µF, U_{bias} = 5.5 kV) is discharged through the pinch coil at t = -42 µs. The orientation of this additional magnetic field is opposite to the main field resulting in magnetic field reconnection at both ends of the pinch coil, which causes axial compression and closed magnetic configuration. Due to an additional inductance (L_{bias} = 6 µH) the quarter period of the bias bank is T/4 = 42 µs, so that the maximum of the bias field is reached just when the main capacitor bank is discharged. At t = -16.2 µs the helium gas is heated up to a few eV by discharging the pre-heating bank (C_{pre} = 1.8 µF, U_{pre} = 40 kV). An ohmic resistor (R_{pre} = 1 MΩ) damps the oscillation decreasing the amplitude to a negligible value when the main discharge is fired. Due to this the bias field is frozen in the pre-ionized helium plasma at $T_e \approx 1...3$ eV and $n_e \approx 5\times10^{16}$ cm^{-3}. The main capacitor bank (C_{main} = 162 µF, U_{main} = 32 kV) connected with the pinch coil (length 60 cm, thickness 7 cm, inner radius 21 cm) is discharged by spark gaps triggered by Marx generators. The plasma parameters that can be achieved with this setup are $T_e \approx 5...50$ eV and $n_e \approx 1\times10^{18}$ cm^{-3}. At t = 5.75 µs the main current is at its maximum (≈ 1.3 MA) and the discharge is crowbarred, i.e. the pinch coil is short circuited, in order to prevent oscillation of the main magnetic field and to achieve lifetimes of the plasma up to 8 µs.

The plasma was diagnosed by means of plasma spectroscopy. Side-on measurements have been performed by a 1:1 imaging of the central plane of the plasma onto the entrance slit of a spectrometer (SPEX model 1704, 1200 lines/mm grating blazed at 550 nm) which is equipped with an optical multichannel analyzer (O-SMA IRY 700G, Princeton Instr.). The plasma continuum radiation at 520 nm has been recorded side-on with a photomultiplier (RCA 1P28A) using a 1/4 m monochromator (Jarrell Ash). The discharge current has been measured by means of a Rogowski-coil that has been placed around the ground plate of the pinch coil. The Rogowski-signal has been monitored with an oscilloscope (Gould DSO 4074, 400 Ms/sec, 100 MHz). End-on measurements have been performed with an ICCD-camera (ICCD-576-G/1, 384×578 pixel of 25 µm^2 each, Princeton Instr.) equipped with an interference filter (λ_0 = 529 nm, $\Delta\lambda$ = 1.1 nm) and an objective (Xenon 1:0.95/50) which results in a spatial resolution of 0.95 mm. The interference filter ensures that only continuum radiation was measured, because no line radiation occurs in the respective wavelength intervall. The gate duration was 40 ns, so that this results in 2-dimensional radially as well as temporally resolved recordings of the plasma continuum radiation along the Z-axis.

The carbon rod (epoxy by Goodfellow) used in the present work is 1 m in length and 3 mm in diameter. It has been positioned on the axis by two mountings inside the discharge tube at a distance of 70 cm from each other, so that the mountings were positioned outside the pinch coil.

End-on measurements with an ICCD-camera

In order to determine the radial distribution of the electron density as well as the compression velocity and the thickness of the shock front the ICCD-camera has been used like an ordinary camera with a gate duration of 40 ns. This has been realized by an MCP, which has been triggered by a pulse generator, so that every end-on photo is a snapshot of the continuum radiation emitted along the Z-axis. A series of 100 photos from 1.0 to 3.5 µs enabled the derivation of all necessary parameters. Fig. 2a shows a typical ICCD photo at t = 1.3 µs. The relative distribution of the electron density has been derived by the well known density dependence of the plasma continuum radiation [2]:

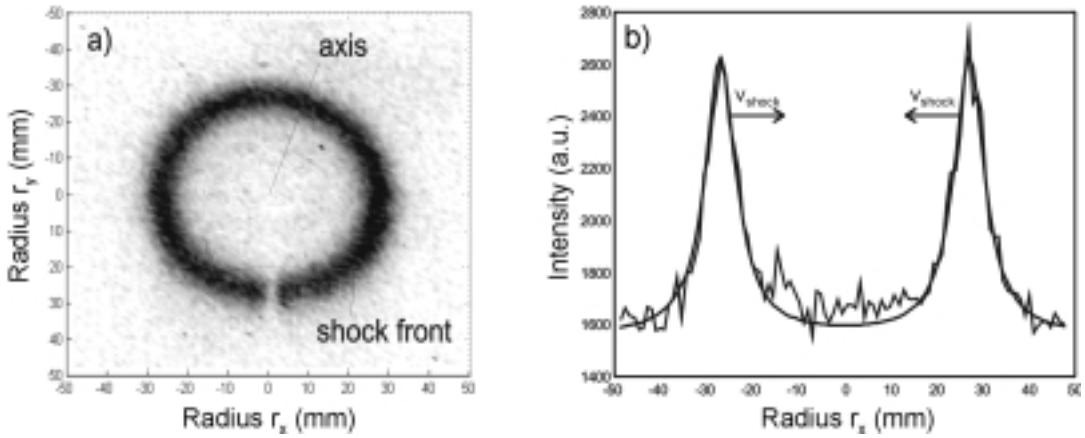

Fig. 2. a) End-on photo of the plasma continuum radiation at $\lambda = 529$ nm taken with the ICCD-camera at $t = 1.3$ µs, b) radial profile of the plasma continuum at $r_y = 0$. The data have been fitted with an analytic function.

$$\varepsilon_{cont} \propto Z_{eff}^2 n_e n_i \quad (1)$$

with the effective charge number Z_{eff} of the ions, the electron density n_e and the ion density n_i. It has been verified by side-on spectroscopy that no impurities occur in the shock front, which means that only HeII ions and electrons are present in the compressing plasma ring. Therefore, $Z_{eff} = 1$, and the emission coefficient of the plasma continuum radiation is proportional to the square of the electron density, because of $n_e = n_i$ (quasi-neutrality). The relative distribution of the electrons and HeII ions along the radius can be derived directly.

As a very helpful result it was found that the radial profile of the electron density can be represented by an analytic expression, which is a function of 3 parameters only: the center, the thickness and the intensity (see Fig. 2b). The distances of the respective centers and the corresponding times of the photos define the compression velocity of the shock front, whereas the width of the radial profile equals the shock front thickness. The results are shown in Fig. 3. It can be seen by the end-on photos (not shown in this paper), that the shock front reaches the carbon rod at $t = 1.5$ µs, and that during the compression the thickness of the shock front remains almost constant ($d = 9$ mm, see Fig. 3a). With respect to the evaluation of the side-on measurements this is of great importance, because the spectroscopic data obtained side-on are spectra which are integrated along the line of sight, so that the radial distribution of the emitters must be known. With a constant thickness the number of free parameters is reduced, which simplifies the evaluation.

The velocity of the compressing shock front is about 50 km/s corresponding to a Mach-number of $M \sim 8$. Using an estimation in [2] this results in an acceleration of the plasma constituents to a velocity of ~37 km/s towards the axis. The Doppler shift due to this compression velocity is about 0.058 nm, which is small compared with the expected Stark-broadening of the HeII P_α (~1.5 nm at $n_e = 5\times10^{17}$ cm^{-3}). Hence, the Doppler shift due to the compression can be neglected in the evaluation of the side-on data.

It should be mentioned that the shape of the shock front is not influenced by the presence of the carbon impurities, but that the compression velocity increases if the carbon rod is added to the device. This can be seen in Fig. 3. The shock front thickness increases when the plasma ring reaches

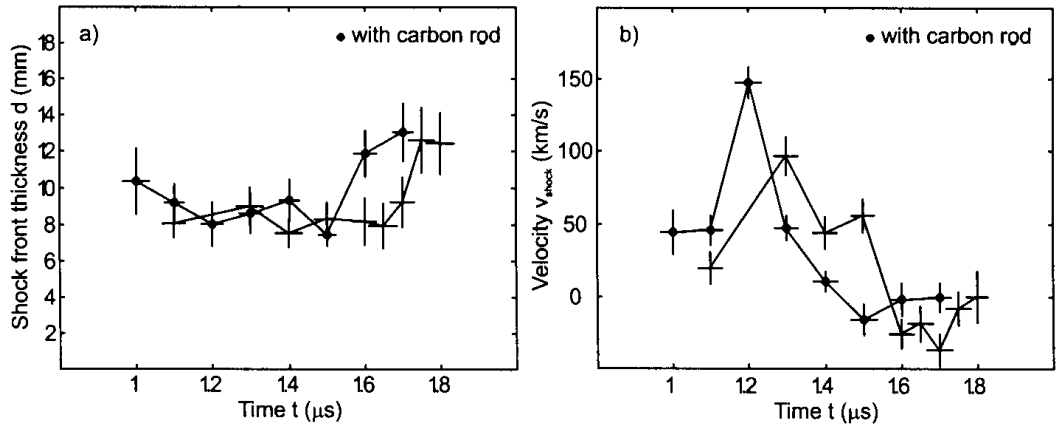

Fig. 3. Shock front thickness (a) and velocity (b) *vs.* time for discharges with and without the rod.

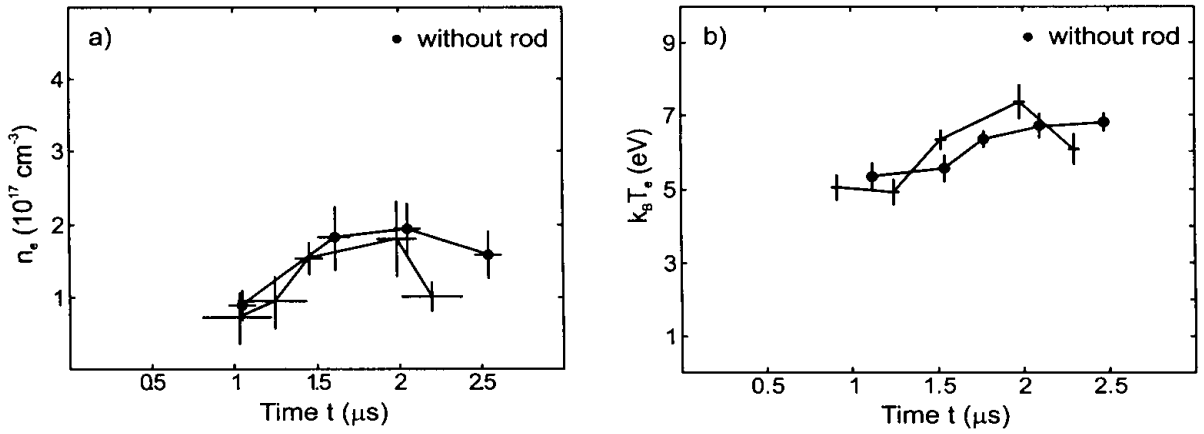

Fig. 4. a) Electron density derived from the Stark broadening of the HeII P_α, b) electron temperature calculated from the relative line intensities of the HeII P_α and the HeI $2p^3P$-$3d^3D$.

the axis. For discharges with the carbon rod this occurs at t ≈ 1.5 μs, while for pure helium discharges the thickness remains constant until t ≈ 1.6 μs. This indicates that the compression to the axis is slower in the latter case. Moreover, the maximum of the compression velocity is 50% higher for discharges with the solid on the axis, and the temporal behaviour is comparable with discharges without the carbon rod, but shifted by 100 ns. An explanation for this is yet to be given.

Side-on measurements with an O-SMA system

Besides laser diagnostics [11] and probe measurements [3, 5], plasma spectroscopy is a well established tool for the analysis of dense plasmas [12, 13]. In particular, the correlation between the electron density and the Stark broadening of the HeII P_α line has been investigated in detail at our Institute comparing experimental results with theoretical predictions for the case of dense, cold plasmas [4]. It was verified that the analytic function given in [14] gives the electron density with high reliability:

$$(2) \qquad n_\varepsilon(\mathrm{cm}^{-3}) = 2.04 \times 10^{16} \times [w_{\mathrm{Stark}}\ (0.1\ \mathrm{nm})]^{1.21}$$

with the electron density ne and the full width at half maximum w_{Stark} of the Lorentzian shape of the Stark broadened line. For the electron temperature T_e we refer to [8], where the dependence of relative line intensities for subsequent ionization stages on the electron temperature has been derived:

$$(3) \qquad \frac{I'}{I} = \frac{f'g'\lambda^3}{fg\lambda'^3} \cdot \exp\left(\frac{E'_\infty - E' - E_\infty + E}{k_B T_e}\right) \cdot \frac{S^z}{\alpha^z}$$

gives the electron temperature to within 10% for densities of $n_e = 10^{16}...10^{18}$ cm^{-3}.

We measured the line profile of the HeII P_α to derive the electron density with eq. (2). The line intensity ratio of the HeII P_α and the HeI $2p^3P$-$3p^3D$ transitions has been measured to calculate the electron temperature with eq. (3). A comparison of the results with those obtained from discharges without the carbon rod on the axis is given in Fig. 4 and demonstrates the influence of the carbon rod on the plasma parameters.

Obviously, the additional carbon ions near the axis result in a drastic lowering of the electron density at t ≥ 2.0 μs. It has already been mentioned that the shock front reaches the axis at t ≈ 1.5 μs, so that it takes about 500 ns of interaction between the helium gas and the carbon solid until an effect can be seen. In contrast to this the influence of the carbon ions on the electron temperature is rather low. Although a weak effect is indicated it should be pointed out that the intensity of the HeI $2p^3P$-$3d^3D$ transition is rather weak for t ≥ 1.8 μs because of a reduced concentration of neutral helium due to ionization.

Conclusion and outlook

The penetration of the shock front through the pre-ionized helium plasma has been observed along the axis with a spatial resolution of 0.95 mm in two dimensions and with a temporal resolution of 100 ns using a fast gated ICCD-camera equipped with an objective and an interference filter transmitting continuum radiation only. The shock front thickness d_{shock} and the velocity v_{shock} have been derived; $d_{\mathrm{shock}} \sim 2$ cm and $v_{\mathrm{shock}} \sim 5\times10^6$ cm/s (which corresponds to a Mach-number of M ~ 8). Comparing discharges with and without the carbon rod on the axis it comes out that the shock front appears earlier (~100 ns), if the carbon rod is on the axis. An explanation remains to be given.

An analytic function for the electron density inside the shock has been derived, which is necessary for the evaluation of the spectroscopic data obtained side-on along the radius. Finally, the shock appears to be of cylindrical symmetry with high accuracy. This is an important point with respect to radially resolved side-on measurements that will be made in the near future, because these data are integrated along the line of sight and, therefore, must be Abel-inverted.

The HeII P_α and HeI $2p^3P^0$-$3d^3D$ transitions were measured side-on at r = 0 in order to obtain the electron density and

temperature in the shock. For discharges with carbon rod the shock front reaches the axis at t ~ 1.5 μs after the main discharge. At t ~ 2.0 μs the electron density starts to decrease from $n_e \sim 1.8\times10^{17}$ to $\sim1\times10^{17}$ cm^{-3}. This delay of ~500 ns agrees with the estimated recombination time of HeII: $\tau \sim$ 300–500 ns at $T_e \sim$ 10–20 eV and $n_e \sim 2\times10^{17}$ cm^{-3} assuming quasi-neutrality.

In order to get a more detailed insight into the physical processes near the axis (i.e. sputtering of carbon from the surface of the solid, ionization and diffusion of carbon impurities in the helium plasma) and the influence on the plasma parameters measurements along the radius with a spectrometer equipped with the ICCD-camera will be carried out. This enables us to measure line profiles at 350 radial positions simultaneously (radial resolution $\delta r = 0.082$ mm by 3:1 imaging) with a gate time of $\Delta t = 20$ ns. Radial profiles of the density of the electrons and ions by means of the width of Stark broadened lines will be derived. Additionally, the occurence of HeI, HeII and CI-CIV lines in combination with the continuum radiation will give information about the physical processes due to the impurities near the axis.

Acknowledgments We thank Dr. Thomas Wrubel and Dr. Stefan Büscher for helpful discussions. This work was supported by the SFB 191 of the German Science Foundation DFG and by INCO-COPERNICUS Contract #ERB IC-15-CT98-0811.

References

1. Armstrong WT, Linford RK, Lipson J, Platts DA, Sherwood EG (1981) Field-reversed experiments (FRX) on compact toroids. Phys Fluids 24:2068–2089
2. Bogen P, Hintz E (1978) Shock induced plasmas. In: Hirsch MN, Oskam JH (eds) Gaseous electronics. Academic Press, New York, pp 453–502
3. Bohm D (1949) In: Guthrie A (ed) The characteristics of electrical discharges in magnetic fields. Wakerling, New York, pp 13–76
4. Büscher St, Glenzer S, Wrubel Th, Kunze H-J (1996) Investigation of the HeII P_α and the HeII P_β transitions at high densities. J Phys B: At Mol Opt Phys 29:4107–4125
5. Chen F (1965) Electric probes. In: Huddlestone RH (ed) Plasma diagnostic techniques. Academic Press, New York, pp 113–200
6. Green TS (1969) Evidence for the containment of a hot, dense plasma in a theta pinch. Phys Rev Lett 5:297–300
7. Greve P, Haumann J, Kunze H-J, Ullrich LK (1982) Effects of an inhomogeneous impurity distribution in a field-reversed theta pinch. Phys Fluids 25;3:452–456
8. Griem HR (1997) Principles of plasma spectroscopy. Cambridge University Press, Cambridge
9. Kolb AC, Dobbie CB, Griem HR (1959) Field mixing and associated neutron production in a plasma. Phys Rev Lett 3:5–7
10. König R, Kolk K-H, Kunze H-J (1987) Influence of impurities on the plasma parameters and stability of a field-reversed configuration. Phys Fluids 30;11:3579–3586
11. Kunze H-J (1968) The laser as a tool for plasma diagnostics. In: Lochte-Holtgreven W (ed) Plasma diagnostics. North-Holland Publishing Company, Amsterdam, pp 550–616
12. Kunze H-J, Kronast B, Freeze W et al. (1996) Diagnostics of plasmas by light scattering. In: Singh RP (ed) Recent advances in plasma science and technology (Plasma 95). Allied Publishers Ltd., New Delhi, pp 139–148
13. Kunze H-J (1997) Selected spectroscopic studies of tokamak plasmas. In: Claaßen H-A (ed) Fourth Workshop on Plasma and Laser Physics, Forschungszentrum Juelich, Bilateral Seminars of the International Bureau. 27:31–45
14. Pitman TL, Fleurier C (1986) Plasma shifts of the HeII H_α and P_α lines. Phys Rev A 33:1291–1296
15. Tuszewski M (1988) Field reversed configuration. Nucl Fusion 28;11:2033–2092